



Characterization of energy conversion of multiferroic PFN and PFN:Mn[#]

Lucjan Kozielski*, Dariusz Bochenek

University of Silesia, Department of Materials Science, 2 Sniezna St., 41-200 Sosnowiec, Poland

Received 26 November 2013; received in revised form 18 December 2013; accepted 23 December 2013

Abstract

Characterization of energy conversion of multiferroic materials is concerned with multifunctional properties of materials, a topic that is fascinating from the scientific point of view and important for the modern technology. The complex characterization of multiferroic structures suffers at present from lack of a systematic experimental approach and deficiency of multifunctional magnetoelectric properties testing capabilities. Compactness and high frequency energy conversion capacity are the main reasons of invention and improvement of sophisticated materials which are prepared for high-speed computer memories and broadband transducer devices. As a consequence, one can easily notice an intense search for new materials for generation, transformation and amplification of magnetic and electric energies. In this scenario, the combination of excellent piezoelectric and magnetic properties makes lead iron niobate $Pb(Fe_{1/2}Nb_{1/2})O_3$ (PFN) an attractive host material for application in integrated magnetoelectric energy conversion applications. PFN multiferroic materials are attractive for commercial electroceramics due to high value of dielectric permittivity and magnetoelectric coefficients as well as relatively easy synthesis process. However, synthesis of PFN ceramics is mostly connected with formation of the secondary unwanted pyrochlore phase associated with dramatic decrease of ferroelectric properties. The authors have successfully reduced this negative phenomenon by Mn doping and finally present high piezoelectric and magnetoelectric energy conversion efficiency in fabricated PMFN ceramics.

Keywords: magnetoelectric effect, PFN ceramics, piezoelectric transformer

I. Introduction

Lead iron niobate, $Pb(Fe_{1/2}Nb_{1/2})O_3$ (PFN) belongs to type-I multiferroics in which ferroelectricity is related to the shift of ferroelectric active d^0 ions (Nb) from the centre of regular oxygen octahedrons - O_6 , while magnetism is related to the presence of d^n iron ions with a natural magnetic moment [1]. The ions of iron (Fe) and niobium (Nb) are substituted randomly at the octahedral B positions in perovskite ABO_3 structure, whereas lead (Pb) goes into the A position. The most important fact is, from the magnetoelectric (ME) coupling point of view, that the angles between the connecting lines of B cation and oxygen are equal to 180 degree, providing optimum conditions for magnetic ordering due to the superexchange interaction.

Admixed PFN ceramic is an interesting material for many electronic and electromechanical applications. In the pure PFN a phase transition from a ferroelectric to paraelectric phase has a diffusive character but adding small amounts of dopants decrease or increase the area of the phase transition. Adding admixtures of elements with similar ionic radii, as Mn, leads to location of these ions in B positions and this is connected with a greater degree of the structure perfection and higher microstructural homogeneity manifested in narrower phase transition area [2]. Admixing PFN with elements of larger ionic radii, such as Sr, K and La, causes widening of the diffusive phase transition area associated with dielectric losses increase [3]. Compared to the non-admixed PFN ceramic, admixed specimens are characterized by a better set of magnetoelectric as well as dielectric parameters and lower dielectric losses.

The influence of the Ba and Ca substitution on ME coefficient has been considered as Pb ions in PFN have leading role in magnetoelectric coupling. In particu-

[#] Paper presented at 10th Conference for Young Scientists in Ceramics - SM-2013, Novi Sad, Serbia, 2013

* Corresponding author: tel: +48 32 3689 564

fax: +48 32 3689 563, e-mail: lucjan.kozielski@us.edu.pl

lar, the decrease of T_N with increase of the Ba doping was explained by possible involvement of the Pb ions in the superexchange of the iron ions [4,5]. Such an influence is observed also for Ti-doped solid solutions of PFN. The Ti-doped PFN phase diagram of the magnetic and ferroelectric properties created on the basis of the piezoelectric, Mossbauer and magnetization data have recently been published [6,7].

Investigation of Mn-doping can also be an interesting topic. Many works have been presented and confirmed the room temperature ferromagnetism in Mn-doped semiconductors. Good example can be ZnO semiconductor, which is also a well-known piezoelectric and electro-optic material, and incorporation of Mn induced ferromagnetism in ZnO that lead to many new multifunctional phenomena. Furthermore, the Mn-doped ZnO material has capability to be produced in powder form with room-temperature multiferroic properties obtained by calcination at temperatures below 500 °C [8]. Above room temperature magnetic transition T_c values have been reported additionally in Mn-doped GaN [9–11] and Ge [12]. Consequently, Mn-doped semiconductors fabrications capability results in new spintronic devices as spin-valve transistors, spin light-emitting diodes, non-volatile memory and logic devices.

Finally, it is important to mention that lower content of pyrochlore phase is associated with above mentioned PFN composition modification and it is possible to obtain pure phase ceramics in simple and non expensive route. For example, lead iron scandium niobate PF-ScN ceramics can be also produced as pure perovskite phase by conventional solid-state reaction method via mixing oxide method (MOM). Dense ceramics (95% of the theoretical density) with optimized dielectric properties can be obtained in air atmosphere high temperature sintering at 1140–1180 °C for 2 h [13]. Similar behaviour has been detected in zinc doped PFN, where at higher values of zinc content ($x > 0.7$), the pyrochlore phase appears but addition of BaTiO₃ suppresses the pyrochlore phase and reduces the magnitude of phase transition area in the relaxor region [14].

The main goal of this work is to examine possible ferroelectric-ferromagnetic coupling increase with associated ME effect enhancement by B position Mn doping of PbFe_{1/2}Nb_{1/2}O₃. Consequently, our work presents a detailed report of the relationships between two samples: one with small pyrochlore phase content and the second with pure perovskite phase Mn-doped considering magnetic field intensity influence on output characteristics. Finally, Mn-doped PMF material with enhanced magnetoelectric properties has been proven practically in magnetic field driven in piezoelectric transformer.

II. Experimental procedure

The preparation of PbFe_{1/2}Nb_{1/2}O₃ (PFN) and Pb(Fe_{1/2}Nb_{1/2})O₃ doped with 1 at.% of Mn (PMFN) ceramics was performed by classical mixed oxide method (MOM) using PbO, Fe₂O₃, Nb₂O₅ and MnO₂ oxides. The milling process was carried out in agate mortar during 8 h time in air atmosphere with subsequent specimens forming by pressing the powders in steel die. The high temperature processing was performed in two stages: i) the first calcination performed at $T_s = 800$ °C for $t_s = 3$ h with subsequent milling and pressing of the powders in steel die, ii) the final high temperature sintering in air at $T = 1125$ °C for 2 h.

The X-ray diffraction profiles of the prepared samples were recorded using PANalytical X'Pert Pro Diffractometer and subsequent phase analysis was performed taking advantage from X'Pert HighScore Plus software. The obtained PFN and PMFN samples microstructure examinations were made using a HITACHI S-4700 SEM. Dielectric measurements were performed on a QuadTech 7600 Plus Precision LCR Meter, in frequency range from 100 Hz to 1 MHz. The hysteresis loops were recorded using the high voltage amplifier Matsusada AMT-5B20 (± 5 kV, 20 mA, <20 kHz). The evaluation of the piezoelectric coefficients were carried out using the resonance -antiresonance method followed by samples poling in silicon oil at 120 °C in electric field of 2 kV/mm. For the magnetoelectric effect measurements the PFN and PMFN samples were placed

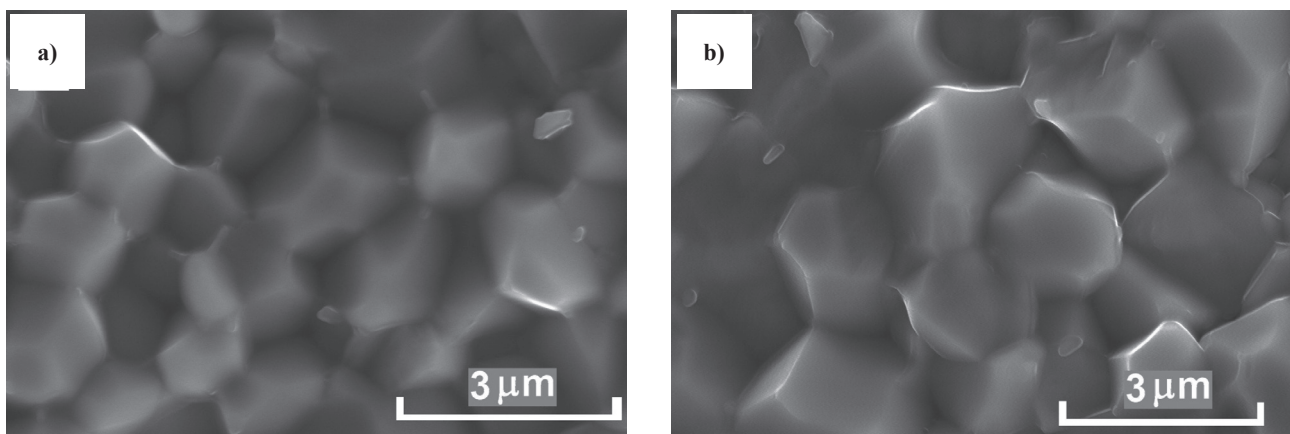


Figure 1. SEM images of: a) PFN and b) PMFN ceramics

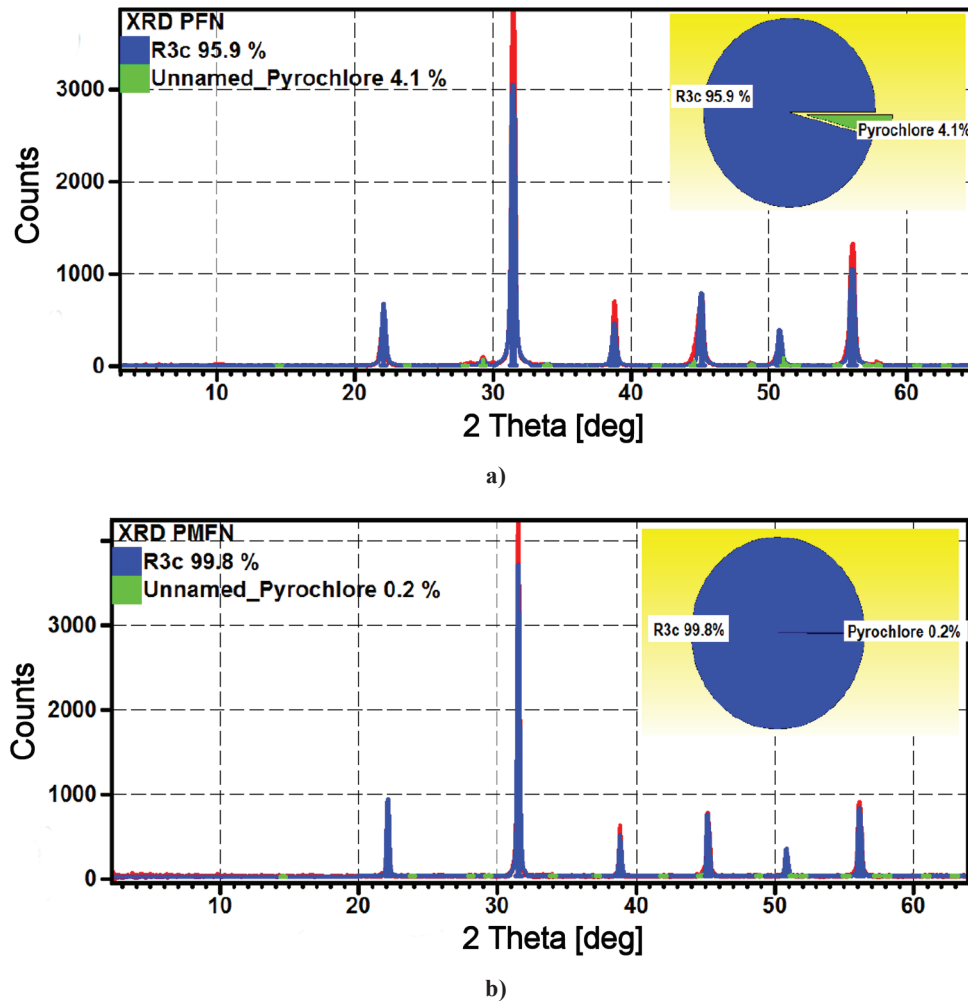


Figure 2. XRD diffraction pattern of: a) PFN and b) PMFN ceramics

in an external constant (H_{DC}) and sinusoidal magnetic field (H_{AC} from 10 Hz to 6.5 kHz) produced by an electromagnet and Helmholtz coils, respectively. The direction of electrical polarization of the samples was directed perpendicularly to both magnetic fields.

III. Results and discussion

3.1 Material testing

The density values of PFN and PMFN ceramics measured by Archimedes method decreased almost imperceptibly from 8.08 to 8.06 g/cm³ respectively. The microstructure and grain size of obtained samples are presented in Fig. 1. The small amount of Mn doping has practically no influence on the average grain size and in both cases well developed grains were found to be uniformly distributed across the samples surfaces. The average grain size of the obtained PFN and PMFN ceramics is about 2.3 μm .

3.2 XRD characterization

The X-ray diffraction patterns of the PFN and PMFN samples with characteristic peaks of perovskite structure are presented in Fig. 2. A rhombohedral $R3c$ space group was assigned to both PFN and PMFN compositions and coexistence of pyrochlore space group for the pure PFN ceramics was traced only in case of the undoped PFN ceramics (Fig. 2a).

It is distinctly visible, that in spite of only one percentage of Mn doping, this has distinctive role in pure perovskite phase formation in the PMFN material. The lattice parameters of the investigated perovskite phases determined by the Rietveld refinement were calculated and listed in Table 1. It can be stated that even addition of a small amount of Mn (1 at.%) in B position of ABO_3 perovskite structure leads to the detectable increase of the a and c unit cell parameters of the PMFN ceramics due to the larger ionic radius of Mn.

Table 1. The parameters of the perovskite unit cell of the investigated ceramics

	a [Å]	b [Å]	c [Å]
PFN	5.6677	5.6677	13.904
PMFN	5.6726	5.6726	13.941

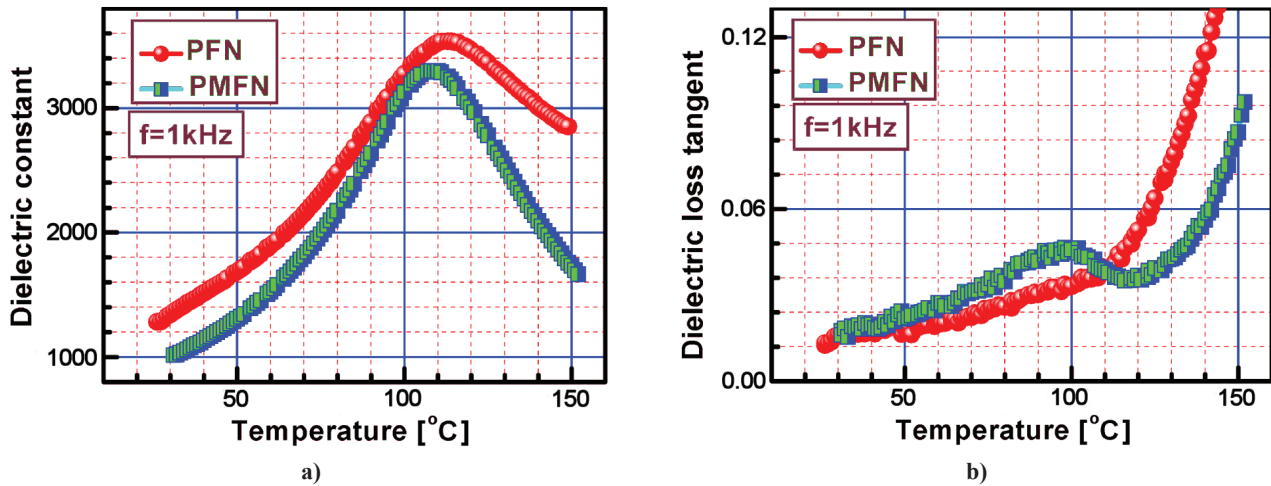


Figure 3. Dielectric permittivity (a) and dielectric loss tangent (b) as a function of temperature at frequency of 1 kHz for PFN and PMFN samples

3.3 Dielectric properties measurement

The temperature dependencies of dielectric permittivity and dielectric losses of both obtained samples were measured at 1 kHz frequency using an Quadtech 7600 LCR Meter for evaluation of Curie temperature of ferroelectric phase transition from rhombohedral to regular (Fig. 3a). The dielectric loss coefficient was measured at 1 kHz by the same method and the measured characteristics are presented in Fig 3b. It is clearly seen, that only 1 at.% of Mn doping plays significant role in the phase transition temperature and character with consequent change of the obtained materials physical properties. The Mn addition caused the Curie temperature shifting from 115 °C to 107 °C with simultaneous drop in dielectric permittivity maximal value from 3300 to 3115 finally associated with less diffused phase transition character.

Generally, a phase transition from a ferroelectric to paraelectric state in PFN has a diffusive character. A wide range of phase transition temperature is related to the degree of structure ordering and arrangement - fill-

ing of iron Fe^{3+} and niobium Nb^{5+} ions (B positions in perovskite ABO_3 structure). The better arrangement, the narrower temperature range of the phase transition is observed so that we can state that adding small amounts of Mn dopant decrease visible the area of the phase transition. Consequently, a location of Mn ions in B position, due to the similar ionic radii, is connected with a greater degree of the structure perfection and higher microstructural homogeneity manifested in narrower phase transition area [2].

A similar tendency connected with structure ordering is also observed in changes of loss tangent. As expected, a diffuse type of phase transition has been observed with no maxima in the range of the phase transition temperatures for the pure PFN (Fig. 3b), but for higher temperature values the shape of dielectric losses curve becomes sharper indicating dramatic conductivity increase. The level of dielectric loss value however, is very low for PFN as well as PMFN samples and is not higher than 0.05 below the T_c indicating good dielectric properties (Fig. 3b).

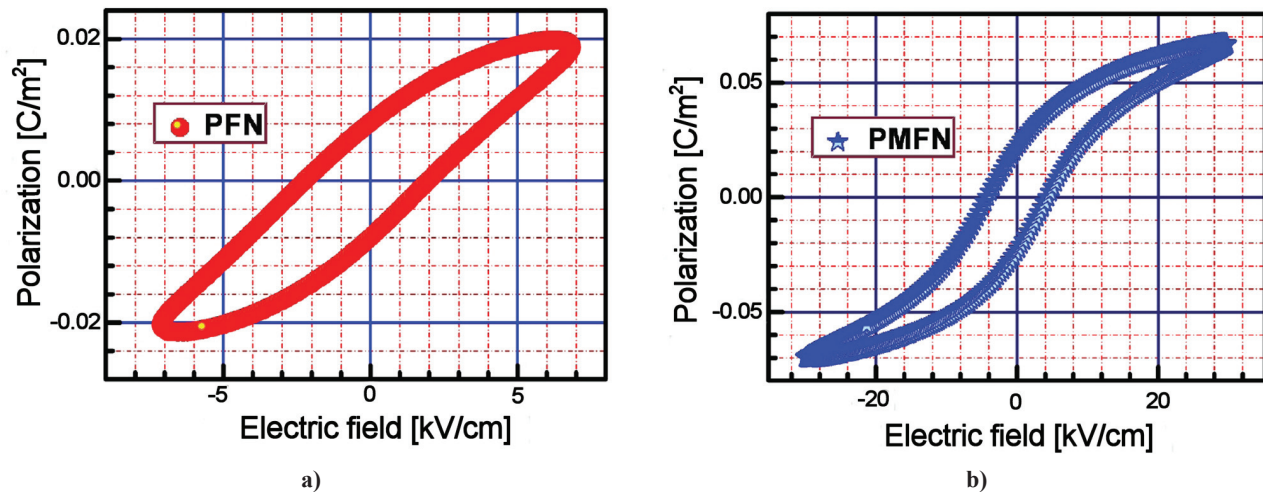


Figure 4. PFN and PMFN ferroelectric hysteresis loops -polarization versus electric field (P-E) curves at room temperature

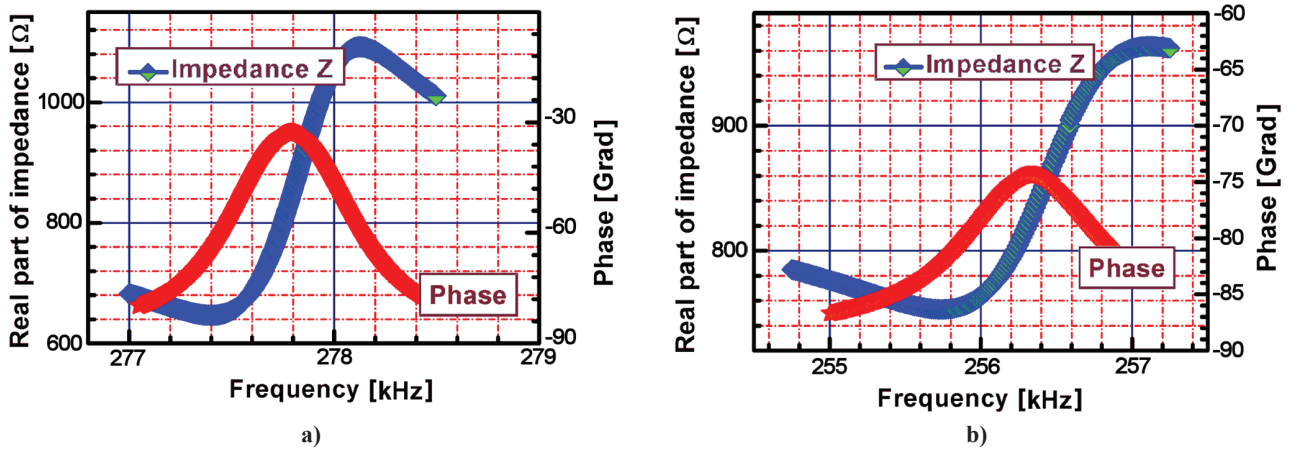


Figure 5. Fundamental electromechanical resonant frequency ranges for PFN (a) and PMFN (b) ceramics at room temperature

In the Fig. 4 the ferroelectric hysteresis loops of PFN and PMFN ceramics are presented. As it was supposed, from the round shape of dielectric permittivity in the vicinity of T_C , PFN composition with small pyrochlore phase content exhibits rounded shape loops whereas, PMFN ceramics has well saturated hysteresis, with relatively low losses and high remanent polarization of 2.5 mC/cm^2 .

3.4 Electromechanical energy conversion efficiency

Measurement of piezoelectric coefficient was done using standard resonance technique (ANSI/IEEE Std 176-1987: IEEE Standard on Piezoelectricity). Recorded characteristic parameters of the fundamental resonant (indicated in Fig. 5) as well as first overtone values were collected and the respective piezoelectric coefficients have been calculated (Table 2). Resonance and antiresonance frequencies were measured together with the static capacitance C_{33}^T of the sample (measured at 1 kHz below piezoelectric resonances).

Taking into account the values of energy conversion parameters presented in Table 2, the Mn doping driven change in piezoelectric coefficients are very significant. Having pyrochlore phase content in mind, the electromechanical performance can be changed only in the case of the phase pure sample. Finally, we can clearly state that even small pyrochlore content can decrease piezoelectric coefficient dramatically (one order of magnitude).

3.5 Magnetolectric energy conversion efficiency

The magnitude of the magnetolectric effect (ME) in PFN ceramics is determined by the measurement set-up presented in Fig. 6a. The change in magnetic polar-

ization causes a bound electric charge, which is present at the domain wall, and this space charge induces an electric field in the electrode surfaces. For the magnetolectric effect induced voltage measurements the PFN and PMFN samples were placed in an external constant (H_{DC}) and sinusoidal magnetic field (H_{AC} from 10 Hz to 6.5 kHz) produced by an electromagnet and Helmholtz coils, respectively. The direction of electrical polarization of the samples was directed perpendicularly to both magnetic fields (Fig. 6a).

After that, the piezoelectric transformers were fabricated from manufactured PFN and PMFN ceramics. The bottom surfaces of disk samples were covered by solid silver electrode, whereas opposite electrode patterns are deposited to create input and output parts separated by 2 mm insulating gaps, with electrodes' area ratio equal 1.66 (Fig. 6b).

The PFN material, due to the coupling between magnetization and polarization became electrically polarized when placed in magnetic field and the induced voltage of 24.3 mV at 1 kHz was recorded (Fig. 7a). This value appeared to be two times higher in the case of PMFN ceramics so that at the last stage of our experiment we have tested the magnetically induced impedance change in the piezoelectric transformer (PT). Investigations of magnetic field influenced properties of PT were essential for our experiment. As it was shown in Fig. 7b the frequency shift of 50 Hz and 20 Ω drop in PT impedance value under 500 Oe magnetic field bias were recorded. Simultaneously, impedance phase shift of 150 Hz is also detectable showing alternative way of magnetic field intensity detection (Fig. 7b). The collect-

Table 2. Electromechanical energy conversion parameters of the investigated ceramics (k_p electromechanical coupling factors for planar vibrations, d_{31} piezoelectric coefficient, Q_m mechanical quality factor, v_R speed of sound in ceramics)

	k_p	d_{31} [C/N]	Q_m	v_R [m/s]
PFN	0.041	$27 \cdot 10^{-12}$	535	2400
PMFN	0.4	$288 \cdot 10^{-12}$	351	2213

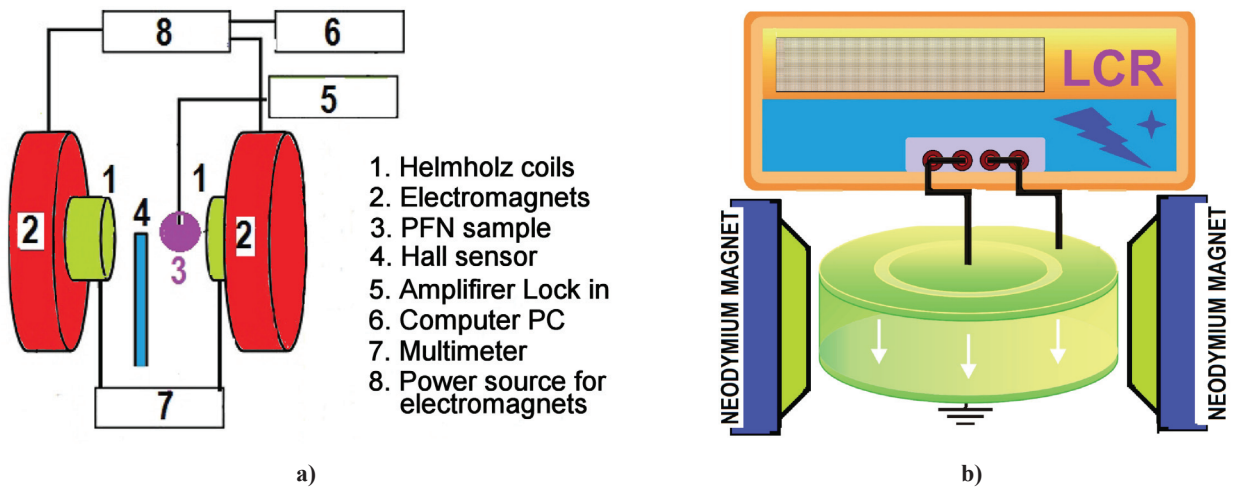


Figure 6. Scheme of Magnetolectric ME coefficient measurements setup (a) and magnetolectric transformer impedance characteristic dependence on magnetic field intensity (b)

ed results proved the high magnetic field-sensing detection capability for the transducer prepared from single phase multiferroic PMFN material.

The explanation of the piezoelectric transformer high sensitivity to magnetic field bias is that this resonant device gives strong response to even small changes in piezoelectric coefficients. Consequently, this device has very narrow impedance characteristics with critical high sensitivity in impedance peaks, so that it can be in such conditions successfully used as magnetic field sensor in such conditions.

IV. Summary

In this paper a new technique of PFN ceramics manganese doping for magnetolectric energy conversion enhancement and corresponding transformer application has been presented. This new method combines the results of the phase transition area decrease from a ferroelectric to paraelectric phase with lowering its diffusive character. A location of Mn ions in B position due

to the similar ionic radius is associated with a greater degree of the structure perfection and higher microstructural homogeneity.

From the piezoelectric energy conversion coefficients evaluation, it is clearly seen that even small percentage of pyrochlore phase plays crucial role in the energy transfer performance and physical properties of obtained materials.

Finally, the authors have been developed a magnetolectric coefficients measurement technique which will provide new information for material engineers who are frequently interested in behaviour of materials within wide range of applied magnetic field. The final efficiently working magnetolectric transformer application will show clearly the response of materials under changing magnetic field in the way that is easily acquired by the engineering society.

Acknowledgments: This work was supported by COST MP0904 Action.

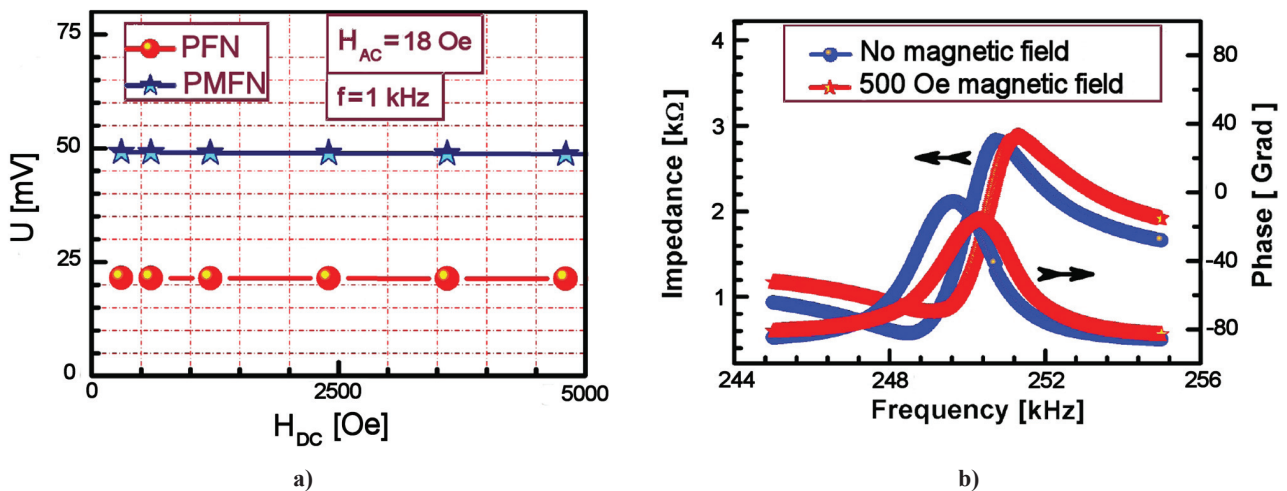


Figure 7. Magnetic field influence on electromagnetic voltage value (a) and on impedance modulus and phase characteristics for PMFN multiferroic material in piezoelectric transformer electrode pattern configuration (b)

References

1. D. Khomskii, "Classifying multiferroics: Mechanisms and effects", *Physics*, **2** (2009) 1–8.
2. D. Bochenek, P. Guzek, "Ferroelectric and magnetic properties of ferroelectromagnetic $\text{PbFe}_{1/2}\text{Nb}_{1/2}\text{O}_3$ type ceramics", *J. Magn. Magn. Mater.*, **323** (2011) 369–374.
3. D. Bochenek, Z. Surowiak, "Influence of admixtures on the properties of biferroic $\text{Pb}(\text{Fe}_{0.5}\text{Nb}_{0.5})\text{O}_3$ ceramic", *Phys. Status Solidi A*, **206** [12] (2009) 2857–2865.
4. I.P. Raevski, S.P. Kubrin, S.I. Raevskaya, V.V. Titov, D.A. Sarychev, M.A. Malitskaya, I.N. Zakharchenko, S.A. Prosandeev, "Experimental evidence of the crucial role of nonmagnetic Pb cations in the enhancement of the Neel temperature in perovskite $\text{Pb}_{1-x}\text{Ba}_x\text{Fe}_{1/2}\text{Nb}_{1/2}\text{O}_3$ ", *Phys. Rev. B*, **80** (2009) 024108 1–6.
5. V.V. Laguta, M.D. Glinchuk, M. Marysko, R.O. Kuzian, S.A. Prosandeev, S.I. Raevskaya, V.G. Smotrakov, V.V. Eremkin, I.P. Raevski, "Effect of Ba and Ti doping on magnetic properties of multiferroic $\text{Pb}(\text{Fe}_{1/2}\text{Nb}_{1/2})\text{O}_3$ ", *Phys. Rev. B*, **87** (2013) 064403 1–8.
6. S.P. Singh, S.M. Yusuf, S. Yoon, S. Baik, N. Shin, D. Pandey, "Ferroic transitions in the multiferroic $(1-x)\text{Pb}(\text{Fe}_{1/2}\text{Nb}_{1/2})\text{O}_3-x\text{PbTiO}_3$ system and its phase diagram", *Acta Mater.*, **58** (2010) 5381–5392.
7. I.P. Raevski, S.P. Kubrin, S.I. Raevskaya, S.A. Prosandeev, M.A. Malitskaya, V.V. Titov, D.A. Sarychev, A.V. Blazhevich, I.N. Zakharchenko, "Dielectric and Mossbauer studies of ferroelectric and magnetic phase transitions in a-site and b-site substituted multiferroic $\text{PbFe}_{0.5}\text{Nb}_{0.5}\text{O}_3$ ", *IEEE Trans. Ultrason. Ferroelectr. Freq. Control*, **59** (2012) 1872–1878.
8. P. Sharma, A. Gupta, K.V. Rao, F.J. Owens, R. Sharma, R. Ahuja, J.M. Osorio Guillen, B. Johansson, G.A. Gehring, "Ferromagnetism above room temperature in bulk and transparent thin films of Mn-doped ZnO", *Nature Mater.*, **2** (2003) 673–677.
9. Y. Matsumoto, M. Murakami, T. Shono, T. Hasegawa, T. Fukumura, M. Kawasaki, P. Ahmet, T. Chikyow, S. Koshihara, H. Koinuma, "Room-temperature ferromagnetism in transparent transition metal-doped titanium dioxide", *Science*, **291** (2001) 854–856.
10. K. Ueda, H. Tabata, T. Kawai, "Magnetic and electric properties of transition-metal-doped ZnO films", *Appl. Phys. Lett.*, **79** (2001) 988–990.
11. G.T. Thaler, M.E. Overberg, B. Gila, R. Frazier, C. R. Abernathy, S.J. Pearton, J.S. Lee, S.Y. Lee, Y.D. Park, Z.G. Khim, J. Kim, F. Ren, "Magnetic properties of n-GaMnN thin films", *Appl. Phys. Lett.*, **80** (2002) 3964–3966.
12. S. Cho, S. Choi, C. Hong, Y. Kim, J. B. Ketterson, B.J. Kim, Y.C. Kim, J.H. Jung, "Ferromagnetism in Mn-doped germanium", *Phys. Rev. B*, **66** (2002) 033303 1–3.
13. B. Fang, Y. Shan, K. Tezuka, H. Imoto, "Phase formation, microstructure and physical properties of lead iron scandium niobate", *J. Eur. Ceram. Soc.*, **26** (2006) 867–873.
14. M.V. Radhika Rao, A.M. Umarji, "Thermal expansion studies in lead iron niobate - Lead zinc niobate and related systems", *Mater. Res. Bull.*, **30** (1995) 1031–1038.

